Polymer 72 (2015) 238–245

Contents lists available at ScienceDirect

Polymer

journal homepage: www.elsevier.com/locate/polymer

RDRP in the presence of Cu^0: The fate of Cu(I) proves the inconsistency of SET-LRP mechanism

Francesca Lorandi, Marco Fantin, Abdirisak Ahmed Isse*, Armando Gennaro*

Department of Chemical Sciences, University of Padova, Via Marzolo 1, 35131 Padova, Italy

ARTICLE INFO

Article history:
Received 24 December 2014
Received in revised form
26 March 2015
Accepted 1 April 2015
Available online 14 April 2015

Keywords:
ATRP
SET-LRP
SARA

ABSTRACT

Metallic Cu in the presence of an amine ligand has become very popular as a catalyst in reversible-deactivation radical polymerization (RDRP). Two contrasting mechanisms were proposed for this process. In SET-LRP, Cu^0 is the exclusive activator, while Cu(I) instantaneously undergoes disproportionation to give Cu(II) and Cu^0. Conversely, in SARA ATRP, Cu^0 plays the role of a supplemental activator as well as a reducing agent for the conversion of Cu(II) to Cu(I), which is the principal activator. One of the cardinal differences between the two mechanisms is whether Cu(I) primarily undergoes disproportionation or reacts with the initiator RX. To provide a clear answer to this question, the kinetics of Cu(I) disproportionation and RX activation were investigated in various experimental conditions that match the polymerization environment (different amine ligands and initiators, effect of solvent, halide ions and Cu^0). In all investigated systems, reaction of Cu(I) with alkyl halides is much faster than disproportionation ($v_{act} > 10^2\ v_{disp}$). This result is in line with SARA ATRP and in clear disagreement with SET-LRP.

1. Introduction

Reversible-deactivation radical polymerization (RDRP) is a powerful technology, which allows polymers to be synthesized with control over the molecular weight and architecture, with tolerance to functional groups and impurities [1–4]. RDRP methods reversibly convert active radicals to dormant chains, thereby gaining control over the macromolecular structure. Among the most popular RDRP methods, ATRP shows a great potentiality and versatility [5–7]. In classical ATRP, a low oxidation state metal complex, for instance Cu(I), reversibly reacts with an alkyl halide to generate a radical and a Cu(II) halide complex [8–11] able to deactivate the radical back to the alkyl halide, as depicted in Fig. 1. Of course, several Cu(I) species are present in the reaction mixture [12], among which, it has been demonstrated that $[Cu^IL]^+$ is the effective activator, whereas $[XCu^IL]$ and $[Cu^IX_2]^-$ are not able to activate the C–X bond [13].

The equilibrium constant, K_{ATRP}, for the activation/deactivation process is generally very low ($10^{-12} - 10^{-4}$), so the concentration of free radicals is quite low ($10^{-9} - 10^{-7}$ M), which means that bimolecular termination is minimized. However, termination cannot be completely avoided and, normally, 1–10% of the chains terminate [14]. This implies the accumulation of a Cu(II) halide complex and slowing down of the polymerization unless a means of regenerating the Cu(I) activator is provided. Several methods for regenerating the Cu(I) complex have been proposed: activator regenerated by electron transfer (ARGET) ATRP [15,16], and initiators for continuous activator regeneration (ICAR) ATRP [17,18], electrochemically mediated ATRP [19–21] and photochemically mediated ATRP [22–25].

Also zerovalent metals have been used for the regeneration of Cu(I) from Cu(II) halide complexes. In particular, Cu^0 was utilized for the first time in RDRP in 1997 [26,27], but recently became popular thanks to the work of Percec's Group who in 2006 published a paper on an efficient RDRP in the presence of Cu^0 [10]. There are several advantages of using Cu^0 in RDRP; these include low concentrations of Cu ions formed during polymerization, control of the polymerization rate through the amount of ligand and Cu^0 surface area, simple removal of the unreacted solid Cu^0 with the possibility of reusing it [11,27–38]. Limiting the quantity of Cu ions to a very low level is highly desirable as it enables preparation of polymeric materials with good purity.

The popular use of Cu^0 in RDRP sparked a vigorous debate on the mechanism of RDRP involving metallic copper, in particular, on the role of Cu^0 and Cu(I) complex [27,39–44]. In 2006 Percec and co-workers [10] proposed a new mechanism, named SET-LRP, which,

* Corresponding authors.
E-mail address: armando.gennaro@unipd.it (A. Gennaro).

http://dx.doi.org/10.1016/j.polymer.2015.04.007
0032-3861/

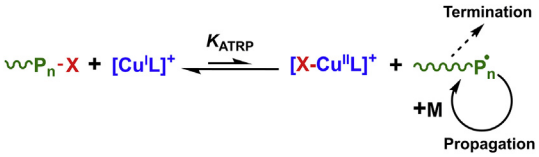

Fig. 1. General mechanism of ATRP.

however, has been significantly modified over the years [43] because several of its assumptions have been demolished by experimental evidences. According to SET-LRP, electron transfer to R-X produces a radical anion $R\text{-}X^{\bullet -}$, which successively undergoes fragmentation of the carbon–halogen bond to give a radical $R^{\bullet}$ and a halide ion X^-. It has been demonstrated that injection of one electron into RX initiators and/or dormant macromolecules P_n-X does not produce radical anions [39], whereas an ion-radical adduct in the solvent cage can be formed when the radical possesses a significant dipolar moment [39,45,46]. Another fundamental assumption of SET-LRP is that Cu^0 is the only activator of C–X bond, but also this assumption has been shown to be wrong. It has been demonstrated that Cu(I) is a more efficient activator than Cu^0, at least by two orders of magnitude [44]. Last, SET-LRP assumes disproportionation of Cu(I) to be fast and complete, but it has recently been shown that disproportionation is neither fast nor complete and that comproportionation is more favored than disproportionation [41].

Since the first successful polymerization of vinyl chloride [47], several papers have been devoted to the use of Cu^0 as promoter of RDRP [48]. Generally, it is assumed that disproportionation is very fast and the so-called "nascent" Cu^0 is very active for the C-X fragmentation, but the role of Cu(I) is ignored. In a recent paper by Haddleton and co-workers [48], Cu^0 was first prepared by disproportionation of Cu(I), then the resulting equilibrium Cu(I)/Cu^0 mixture was subsequently reacted with the initiator and the monomer, obtaining good conversion and control of polymerization. This good performance was attributed exclusively to the Cu^0 formed by disproportionation without considering the quantity of Cu(I), which might not be negligible, remaining after the disproportionation reaction reached equilibrium. In addition, when Cu^0 reacts with RX, it generates Cu(I). Thus, even if the process starts with a negligible amount of Cu(I), the presence of this species during polymerization cannot be ignored. Therefore, a better comprehension, without preconceptions, of the role of Cu(I) is required.

Since it has been demonstrated that a Cu wire is not more active than Cu(I) toward C–X activation, the supporters of SET-LRP mechanism argue that "nascent" Cu^0, arising from disproportionation of Cu(I), reacts with R–X faster than Cu(I), whose principal role in the reaction mixture is therefore the continuous regeneration of "nascent" Cu^0. Note, however, that "nascent" Cu^0 cannot activate R–X faster than its formation by disproportionation of Cu(I). So the real question is, does Cu(I) undergo disproportionation faster than its reaction with the initiator? The aim of this work is to provide a clear answer to this key question in the debate on the mechanism of RDRP in the presence of metallic Cu. The investigation was carried out in DMSO, which has been defined, "an excellent solvent for SET [where] the nascent Cu^0 generated by the disproportionation is rapidly consumed upon addition of 2-bromopropionate" [43]. A wide range of experimental conditions typically used for RDRP with Cu^0 were considered: MA/DMSO 2/1 (v/v) (MA = methyl acrylate) as reaction medium, Me_6TREN and TPMA as ligands, MCP, BC, EBA, EBiB as initiators (Fig. 2).

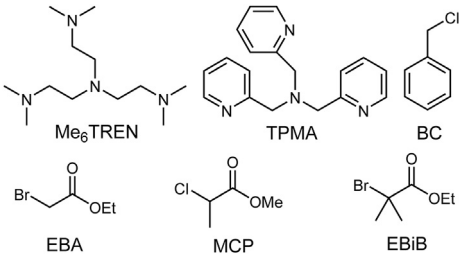

Fig. 2. Chemical structures of investigated amine ligands and initiators.

2. Experimental

2.1. Materials

Dimethyl sulfoxide (DMSO, VWR anhydrous, 99.9+%), tris[2-(dimethylamino)ethyl]amine (Me_6TREN, Sigma–Aldrich, 98%), tri(2-pyridylmethyl)amine (TPMA, Sigma–Aldrich, 98%), copper(II) trifluoromethanesulfonate ($Cu^{II}(OTf)_2$, Aldrich, 98%), or tetrakis(acetonitrile)copper(I) tetrafluoroborate ($Cu^{I}(MeCN)_4BF_4$, Sigma–Aldrich, 97%), ethyl bromoacetate, benzyl chloride, methyl 2-chloropropionate and ethyl 2-bromoisobutyrate (all from Sigma–Aldrich, >98%) were used as received. Immediately before use, Cu^0 (wire, diameter 1.0 mm, Alfa Aesar, 99.9%) was washed with MeOH/HCl (3/1) and then with fresh MeOH and DMSO. In a few cases the Cu wire was activated by treatment with hydrazine monohydrate ($NH_2NH_2{\bullet}H_2O$, Sigma-Aldrich, 98%) and then washed with DMSO before use [49]. Tetraethylammonium tetrafluoroborate (Et_4NBF_4, Alfa Aesar, 99%), used as supporting electrolyte, was recrystallized from ethanol and dried in a vacuum oven at 70 °C for 48 h. Tetraethylammonium bromide (Et_4NBr, Sigma–Aldrich, 99%) and tetraethylammonium chloride (Et_4NCl, Sigma–Aldrich, 98%) were recrystallized from ethanol and ethanol/diethyl ether, respectively, and dried at 70 °C under vacuum for 48 h.

A stock solution (ca 0.2 M in CH_3CN) of tetrakis(acetonitrile) copper(I) tetrafluoroborate ($Cu^{I}(MeCN)_4BF_4$) was prepared in a drybox and standardized by spectrophotometric analysis, using 2,9-dimethyl-1,10-phenanthroline as a specific ligand ($\varepsilon = 8458\ M^{-1}\ cm^{-1}$) in a 2-fold excess with respect to the metal [50]. All Cu(II) complexes were always prepared in situ starting from copper(II) trifluoromethanesulfonate.

2.2. Instrumentation

Cyclic voltammetry experiments were carried out in a three-electrode cell by using an Autolab PGSTAT 30 potentiostat/galvanostat (EcoChemie, The Netherlands) run by a PC with GPES software. A glassy carbon (GC) disk, fabricated from a 3 mm diameter GC rod (Tokai GC-20), and a Pt ring were used as working electrode and counter electrode, respectively. Prior to each experiment the working electrode surface was cleaned by polishing with a 0.25-μm diamond paste, followed by ultrasonic rinsing in ethanol for 5 min. The reference electrode was Ag|AgI|0.1 M *n*-Bu_4NI in DMF, which was always calibrated at the end of each experiment against the ferrocenium/ferrocene couple. The standard potential of this couple in DMSO and MA/DMSO 2/1 (v/v) was measured as 0.449 V and 0.495 V vs SCE (saturated calomel electrode), respectively, which allowed conversion of all measured potentials to the SCE scale. To avoid diffusion of I^- into the working solution, the reference electrode was separated from the working solution compartment by a double bridge made of a glass frit and a Et_4NBF_4-saturated methyl

cellulose gel. The first bridge was filled with 0.1 M *n*-BuNI in DMF, whereas the second one contained the working medium.

The kinetics of Cu(I) disproportionation and of the reaction between RX and Cu(I) were studied by monitoring the concentration of Cu(I) at a rotating disk electrode (RDE, Autolab, Eco-Chemie) with a GC tip disc (3 mm diameter, Metrohm).

All electrochemical investigations were carried out at 25 °C and the solutions ($V = 15$ mL) were always degassed with an argon flow for 30 min prior to each experiment.

3. Results and discussion

3.1. Cyclic voltammetry

Copper(II) complexes with polyamine ligands such as Me_6TREN and TPMA undergo quasi-reversible one electron transfer to the corresponding Cu(I) complexes [12,51,52]. An example of typical voltammetric responses of Cu^{2+}, $[Cu^{II}L]^{2+}$ and $[ClCu^{II}L]^{+}$ is reported in Fig. 3. The peak couple observed for the reduction of Cu^{2+} shifts to more negative potentials after addition of TPMA; further addition of X^- (X = Cl, Br) causes further negative shift of the peak couple. A similar behavior was observed for all other Cu/L/X combinations in both DMSO and MA/DMSO. In all cases, the peak couple is due to the reversible reduction of Cu(II) to Cu(I) (eqs. (1)–(3)), but the identity of the redox couple changes with the added ligand(s).

$$Cu^{2+} + e^- \rightleftharpoons Cu^{+} \tag{1}$$

$$\left[Cu^{II}L\right]^{2+} + e^- \rightleftharpoons \left[Cu^{I}L\right]^{+} \tag{2}$$

$$\left[ClCu^{II}L\right]^{+} + e^- \rightleftharpoons \left[ClCu^{I}L\right] \tag{3}$$

The standard potential of the Cu(II)/Cu(I) couple can be estimated as $E^{\ominus} \approx E_{1/2} = (E_{pc} + E_{pa})/2$, where E_{pc} and E_{pa} are the cathodic and anodic peak potentials, respectively. Values of $E^{\ominus}$ estimated for all complexes from cyclic voltammetry are listed in Table 1. Both Cu(II) and Cu(I) form stable binary complexes with amine ligands (L) and ternary complexes when both L and halide ions X^- are present in solution. $E^{\ominus}$ of the $[Cu^{II}L]^{2+}/[Cu^{I}L]^{+}$ couple can be related to that of the uncomplexed Cu^{2+}/Cu^{+} couple and the stability constants of $[Cu^{II}L]^{2+}$ and $[Cu^{I}L]^{+}$, β^{II} and β^{I}, respectively (eq. (4)).

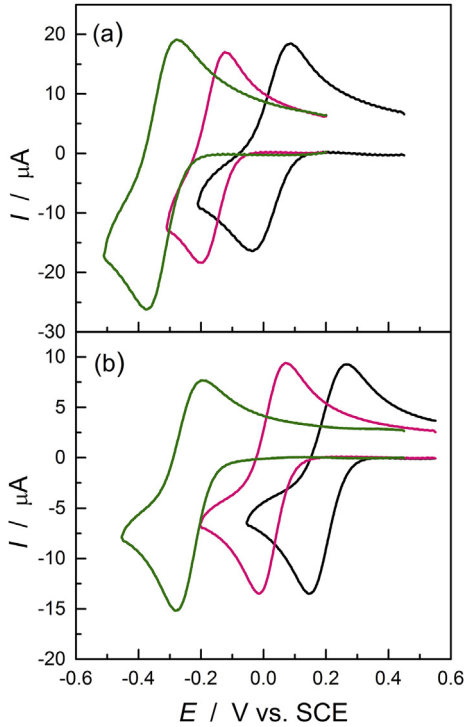

Fig. 3. From right to left, CV curves of $Cu^{II}(OTf)_2$, $[Cu^{II}TPMA]^{2+}$ and $[ClCu^{II}TPMA]^{+}$ in (a) DMSO and (b) MA/DMSO 2/1 (v/v), containing 0.1 M Et_4NBF_4; $v = 0.2$ V/s; $T = 25$ °C.

$$E^{\ominus}_{[Cu^{II}L]^{2+}/[Cu^{I}L]^{+}} = E^{\ominus}_{Cu^{2+}/Cu^{+}} + \frac{RT}{F}\ln\frac{\beta^{I}}{\beta^{II}} \tag{4}$$

A similar relationship exists between the standard reduction potentials of $[Cu^{II}L]^{2+}$ and $[XCu^{II}L]^{+}$:

$$E^{\ominus}_{[XCu^{II}L]^{+}/[XCu^{I}L]} = E^{\ominus}_{[Cu^{II}L]^{2+}/[Cu^{I}L]^{+}} + \frac{RT}{F}\ln\frac{K^{I}_{X}}{K^{II}_{X}} \tag{5}$$

where K^{I}_{X} and K^{II}_{X} are the equilibrium constants of the association of X^- with $[Cu^{I}L]^{+}$ and $[Cu^{II}L]^{2+}$, respectively. The direction and extent of $E^{\ominus}$ shift with respect to $E^{\ominus}_{Cu^{2+}/Cu^{+}}$ depend on the values of β^{I}/β^{II} and K^{I}_{X}/K^{II}_{X}. Equations (4) and (5) were used to calculate the relative stability constants and halidophilicities of $[Cu^{II}L]^{2+}$ and $[Cu^{I}L]^{+}$ and the observed values of β^{I}/β^{II} and K^{I}_{X}/K^{II}_{X} are reported in Table 1. The separate values of β^{I}, β^{II}, K^{I}_{X} and K^{II}_{X} are not known and could not be calculated here, but the reported ratios could be used to calculate them when at least one value of each couple becomes available. As shown in Table 1, both β^{I}/β^{II} and K^{I}_{X}/K^{II}_{X} are much smaller than unity both in DMSO and MA/DMSO, clearly indicating that in all investigated

Conditions Cu(II) complexes are more stable than their respective Cu(I) complexes. The higher stability of Cu(II) than Cu(I) is reflected on the standard potentials of the Cu(II)/Cu(I) couple, which show the trend: $E^{\ominus}_{[XCu^{II}L]^{+}/[XCu^{I}L]} < E^{\ominus}_{[Cu^{II}L]^{2+}/[Cu^{I}L]^{+}} < E^{\ominus}_{Cu^{2+}/Cu^{+}}$.

3.2. Kinetics of Cu(I) disproportionation

Although the stability constants of $[Cu^{I}L]^{+}$ and $[XCu^{I}L]$ in DMSO and MA/DMSO are not known, it is likely that $[Cu^{I}L]^{+}$ is the only species present in solution when L is the only ligand in solution, whereas both species will be formed in the presence of both L and X^-. Lack of knowledge on the stability constants precludes any possibility of calculations on Cu(I) speciation and hence identification of predominant species that may be undergoing disproportionation. It is important to stress, however, that when different Cu(I) species are present, for instance $[Cu^{I}L]^{+}$, $[XCu^{I}L]$, $[Cu^{I}X_2]^{-}$, etc, one has to consider all possible reactions between these species. The overall disproportionation reaction will be made up of different contributions from a series of parallel reactions between Cu(I) species. Thus, even if one were able to compute precise speciation of Cu(I), this would hardly be of any help to determine separate disproportionation rate constants for the various possible reactions.

Faced with these difficulties, we decided to measure the overall rate constant of disproportionation. Additionally, we consider disproportionation to be principally occurring in solution, especially in the initial stages of the reaction where the surface of Cu^0 is very small. In a previous study [41], data on equilibrium and rate constants of comproportionation, K_{comp} and k_{comp}, were used to estimate disproportionation rate constants. In that context, an apparent diproportionation rate constant was defined as $k^{app}_{disp} = k^{app}_{comp}/K_{comp}$ and was expressed in cm s^{-1}, that is, the same units of k^{app}_{comp}. Although we are aware that disproportionation can occur also by a heterogeneous process involving Cu^0, we will analyze the reaction kinetics as a homogeneous process and assess

Table 1
Some thermodynamic data for Cu(I) and Cu(II) complexes in DMSO and MA/DMSO 2/1 (v/v) + 0.1 M Et_4NBF_4 at 25 °C.

Entry	Redox couple	Solvent	L	$E^{\ominus}$ (V vs SCE)	β^{I}/β^{II} [a]	K_X^I/K_X^{II} [b]
1	Cu^{2+}/Cu^{+}	DMSO	– [c]	0.048		
2	$[Cu^{II}L]^{2+}/[Cu^{I}L]^{+}$	DMSO	Me_6TREN	−0.251	8.8×10^{-6}	
3	$[Cu^{II}L]^{2+}/[Cu^{I}L]^{+}$	DMSO	TPMA	−0.156	3.6×10^{-4}	
4	$[ClCu^{II}L]^{+}/[ClCu^{I}L]$	DMSO	Me_6TREN	−0.428		1.0×10^{-3}
5	$[BrCu^{II}L]^{+}/[BrCu^{I}L]$	DMSO	Me_6TREN	−0.347		2.5×10^{-2}
6	$[ClCu^{II}L]^{+}/[ClCu^{I}L]$	DMSO	TPMA	−0.340		7.8×10^{-4}
7	Cu^{2+}/Cu^{+}	MA/DMSO	– [c]	0.202		
8	$[Cu^{II}L]^{2+}/[Cu^{I}L]^{+}$	MA/DMSO	Me_6TREN	−0.128	2.6×10^{-6}	
9	$[Cu^{II}L]^{2+}/[Cu^{I}L]^{+}$	MA/DMSO	TPMA	0.032	1.3×10^{-3}	
10	$[ClCu^{II}L]^{+}/[ClCu^{I}L]$	MA/DMSO	Me_6TREN	−0.367		9.1×10^{-5}
11	$[BrCu^{II}L]^{+}/[BrCu^{I}L]$	MA/DMSO	Me_6TREN	−0.311		8.1×10^{-4}
12	$[ClCu^{II}L]^{+}/[ClCu^{I}L]$	MA/DMSO	TPMA	−0.254		1.5×10^{-5}

[a] β^{I} and β^{II} are the equilibrium constants of the reactions $Cu^{+} + L \rightleftharpoons [Cu^{I}L]^{+}$ and $Cu^{2+} + L \rightleftharpoons [Cu^{II}L]^{2+}$, respectively.
[b] K_X^I and K_X^{II} are the equilibrium constants of the reactions $[Cu^{I}L]^{+} + X^{-} \rightleftharpoons [XCu^{I}L]$ and $[Cu^{II}L]^{2+} + X^{-} \rightleftharpoons [XCu^{II}L]^{+}$, respectively.
[c] Without any added ligand.

the effect of Cu^0 wire on k_{disp}. The general disproportionation reaction of Cu(I) species present in solution can be expressed as

$$2Cu(I) \rightleftharpoons Cu(II) + Cu^0 \quad (6)$$

Investigations on the kinetics of disproportionation were performed by monitoring the concentration of Cu(I) on a rotating disc electrode (RDE), operating at a fixed angular velocity (ω) and a constant applied potential, E_{app}, of 0.2 V. This value is significantly more positive than $E_{1/2}$ of all the relevant copper complexes present in solution (see Fig. 3), so that all Cu(I) species undergo oxidation at the electrode. The oxidation process at this potential is under diffusion control and the measured limiting current, I_L, is correlated to the bulk concentration of Cu(I), $C_{Cu(I)}$, thorough the Levich equation [53]:

$$I_L = 0.62nFAD^{2/3}\omega^{1/2}\nu^{-1/6}C_{Cu(I)} \quad (7)$$

where n is the number of exchanged electrons, F is the faraday constant, D is the diffusion coefficient of Cu(I) species undergoing oxidation, A is the area of the electrode and ν is the kinematic viscosity.

The reaction rate can be expressed as the rate of disappearance of Cu(I):

$$-\frac{dC_{Cu(I)}}{dt} = 2k_{disp}C_{Cu(I)}^2 \quad (8)$$

which upon integration gives the kinetic rate law:

$$\frac{1}{C_{Cu(I)}} - \frac{1}{C_{Cu(I)}^0} = 2k_{disp}t \quad (9)$$

where $C_{Cu(I)}^0$ is the initial concentration of Cu(I).

The experiments for k_{disp} determination were usually started by applying a constant potential of 0.2 V vs SCE to the RDE (ω = 2500 rpm) in a stirred solution containing the ligand but without copper. Cu(I) was then introduced and immediately an anodic current was observed, which decayed with time owing to the disproportionation reaction. The limiting current, I_L^0, measured at the moment in which Cu(I) is introduced ($t = 0$) is related to the initial concentration of Cu(I), $C_{Cu(I)}^0$ through the Levich equation (Eq. (7)). The same equation can be applied to the decaying current measured during the disproportionation reaction. It follows then that the concentration of Cu(I) as a function of time is given by

$$C_{Cu(I)} = \frac{I_L}{I_L^0}C_{Cu(I)}^0 \quad (10)$$

Examples of the decrease of Cu(I) with time together with the corresponding linear plots based on equation (9) are reported in Fig. 4. It is important to note that only the first 150–300 s of the reaction were analyzed with the linear regression to determine k_{disp}. This short reaction time was chosen to avoid possible contribution of the inverse comproportionation reaction to the overall reaction rate and also to prevent significant consumption of Cu(I) by the oxidation process at the electrode. In fact, both comproportionation and Cu(I) consumption by electrooxidation become relevant at much longer times. The disproportionation rate constants determined for the Cu(I) complexes, both in DMSO and MA/DMSO are summarized in Table 2. It is worth noting that in general these disproportionation experiments did not give highly reproducible results, therefore all reported k_{disp} values were obtained as the average of three replicas.

According to the data reported in Table 2, disproportionation of Cu(I) in DMSO or MA/DMSO is not a fast reaction. However, the presence of metallic copper in the reaction environment may significantly enhance the disproportionation rate, via heterogeneous catalysis at the metal surface [27,41]. Therefore, we measured k_{disp} in the presence of a Cu wire; immediately before use, the wire was activated by either treatment with HCl/MeOH solution or hydrazine reduction. The measured rate constants, which were independent of the activation mode within experimental error, are collected in Table 3. As shown, k_{disp} increases with increasing metal surface, but the presence of Cu^0 does not dramatically affect the overall rate of the process. In both investigated reaction media the presence of a 30 cm Cu wire (surface area = 9 cm^2) increases k_{disp} roughly by a factor of two.

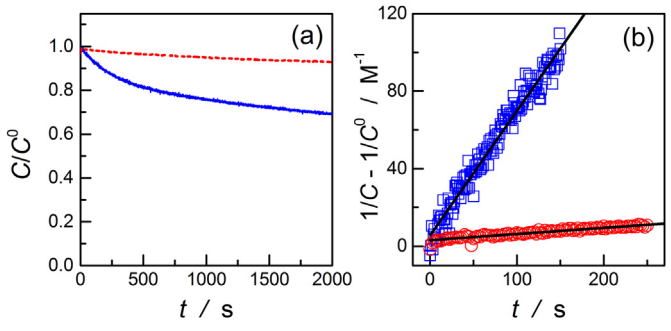

Fig. 4. (a) Decay of Cu(I) concentration in DMSO + 0.1 M Et_4NBF_4, recorded for 10^{-3} M $[Cu^{I}Me_6TREN]^{+}$ in the absence (solid line) and presence (dashed line) of 2×10^{-3} M Et_4NBr at 25 °C. (b) Kinetic analysis according to a second-order rate law, carried out in the absence (□) and presence (○) of Br^{-}.

Table 2
Disproportionation rate constants, k_{disp}, in DMSO and MA/DMSO 2/1 (v/v) + 0.1 M Et_4NBF_4 at 25 °C. $C_{Cu(I)} = 10^{-3}$ M, $C_{Cu(I)}$:C_L = 1:1.1. Accuracy ± 20%.

Entry	L	X⁻[a]	k_{disp}/M^{-1} s^{-1}	
			DMSO	MA/DMSO 2/1
1	Me_6TREN	–	1.2	0.77
2	Me_6TREN	Br^-	0.062	0.61
3	Me_6TREN	Cl^-	0.057	0.57
4	TPMA	–	0.37	0.94
5	TPMA	Cl^-	0.13	0.20

[a] Added as Et_4NCl or Et_4NBr; when present, C_{X^-}:$C_{Cu(I)}$ = 2:1.

Table 3
Disproportionation rate constants, k_{disp}, of 10^{-3} M Cu(I) in DMSO and MA/DMSO 2/1 (v/v) + Et_4NBF_4 0.1 M at 25 °C, in the presence of Me_6TREN and a copper wire (diameter = 1 mm). $C_{Cu(I)}$ = 1 mM, $C_{Cu(I)}$:C_{Me_6TREN} = 1:1.1. Accuracy ± 20%.

Entry	X⁻[a]	l_{wire}/cm	k_{disp}/M^{-1} s^{-1}	
			DMSO	MA/DMSO 2/1
1	–	10	1.4	1.3
2	–	20	2.6	1.4
3	–	30	2.7	1.7
4	Cl^-	20	0.13	0.70
5	Br^-	20	0.047	0.65

[a] Added as Et_4NCl or Et_4NBr; when present, C_{X^-}:$C_{Cu(I)}$ = 2:1.

This moderate k_{disp} increase, albeit confirming the catalytic role of Cu^0, points out that the disproportionation reaction principally occurs in the homogeneous phase.

3.3. Kinetics of RX activation by Cu(I)

The reaction between Cu(I) and RX is fast, but, as previously mentioned, the ATRP equilibrium is strongly shifted toward the reactants and in normal conditions the fraction of converted Cu(I) is very low, preventing the possibility of obtaining any kinetic information by simply mixing Cu(I) and RX. To overcome this difficulty, the radical scavenger 2,2,6,6-tetramethyl-1-piperidinyloxy (TEMPO) was used in a large excess with respect to Cu(I), allowing quantitative and irreversible trapping of R$^\bullet$. The rate constant of radical trapping by nitroxides is typically close to the diffusion-controlled limit [54,55], so that the overall process (Eqs. (11) and (12)) can be considered to be irreversible and kinetically controlled by the activation reaction, which is considered to be due to $[Cu^IL]^+$ [13]:

$$[Cu^IL]^+ + RX \rightleftharpoons [XCu^{II}L]^+ + R^\bullet \quad (11)$$

$$R^\bullet + TEMPO \rightarrow R{-}TEMPO \quad (12)$$

Another important issue that should be taken into account is that besides activating RX, Cu(I) is always engaged in a disproportionation reaction. For all investigated systems, a comparison between the decay rates of Cu(I) in the absence and presence of RX has shown that RX activation is much faster than disproportionation. As shown in Fig. 5, which exemplifies such a comparison, the lifetime of Cu(I) is drastically reduced when RX is added to a solution of Cu(I) in DMSO or MA/DMSO; disproportionation reactions required hours to approach equilibrium, whilst activation reactions lasted within few minutes. Therefore, activation kinetics can be studied by monitoring the disappearance of Cu(I) at a rotating disc electrode (RDE), neglecting the contribution of disproportionation to the overall rate of Cu(I) decay.

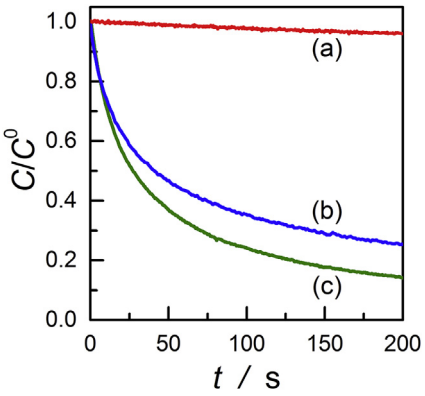

Fig. 5. Decay of Cu(I) in MA/DMSO 2/1 (v/v) + 0.1 M Et_4NBF_4 at 25 °C: (a) 10^{-3} M $[Cu^IMe_6TREN]^+$ + 2 × 10^{-3} M Et_4NBr; (b) 5 × 10^{-4} M $[Cu^IMe_6TREN]^+$ + 10^{-3} M Et_4NCl + 10^{-2} M BC + 10^{-2} M TEMPO; (c) 10^{-3} M $[Cu^IMe_6TREN]^+$ + 2 × 10^{-3} M Et_4NBr + 10^{-3} M EBA + 2 × 10^{-2} M TEMPO.

Two kinetic regimes were used to determine k_{act}. For relatively slow reactions, the activation kinetics can be examined under pseudo-first-order conditions, that is, using $C^0_{RX}/C^0_{[Cu^IL]^+} \geq 20$. The rate of disappearance of $[Cu^IL]^+$ in this circumstance can be expressed as:

$$-\frac{dC_{[Cu^IL]^+}}{dt} = k_{act}C_{[Cu^IL]^+}C_{RX} = k'C_{[Cu^IL]^+} \quad (13)$$

which upon integration gives

$$\ln C_{[Cu^IL]^+} = \ln C^0_{[Cu^IL]^+} - k't \quad (14)$$

where $k' = k_{act}C^0_{RX}$.

For fast reactions, second-order conditions were chosen. If the reaction is performed using $C^0_{[Cu^IL]^+} = C^0_{RX}$, the kinetic rate law becomes:

$$\frac{1}{C_{[Cu^IL]^+}} - \frac{1}{C^0_{[Cu^IL]^+}} = k_{act}t \quad (15)$$

In both cases, the limiting current is measured and converted to $C_{[Cu^IL]^+}$ using equation (10).

Analyses of RX activation kinetics according to equations (14) and (15) have shown linear plots from which k_{act} was extracted through regression analysis. Examples of linear plots based on equations (14) and (15) are reported in Fig. 6, whereas the

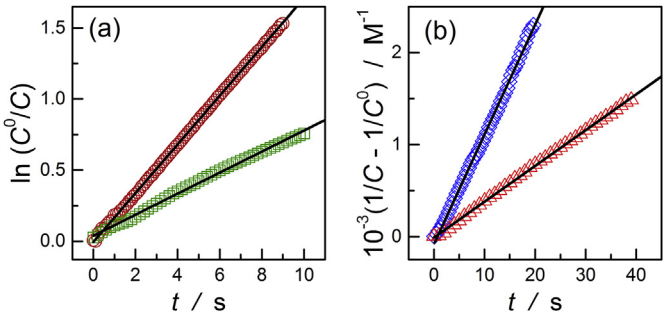

Fig. 6. Kinetic analysis of RX activation at 25 °C in MA/DMSO 2/1 (v/v) + 0.1 M Et_4NBF_4 in the presence of (a) 10^{-2} M TEMPO, according to a pseudo-first-order rate law or (b) 5 × 10^{-3} M TEMPO, according to a second-order rate law: (○) 5 × 10^{-4} M $[Cu^IMe_6TREN]^+$ + 10^{-2} M BC; (□) 5 × 10^{-4} M $[Cu^ITPMA]^+$ + 10^{-3} M Et_4NCl + 10^{-2} M MCP; (◇) 5 × 10^{-4} M $[Cu^IMe_6TREN]^+$ + 5 × 10^{-4} M EBA; (△) 5 × 10^{-4} M $[Cu^IMe_6TREN]^+$ + 10^{-3} M Et_4NBr + 5 × 10^{-4} M EBA.

activation rate constants determined for several systems are summarized in Table 4. In RDRP experiments with Cu^0, often $Cu^{II}X_2$ is added together with the amine ligand. Therefore, the effect of X^- was examined. As shown in Table 4, the presence of X^- in a two-fold excess with respect to Cu(I) has the effect of slowing the activation rate, because of the formation of inactive $[XCu^{I}L]$ and $[Cu^{I}X_2]^-$ species [13]. The effect of X^- is higher for Cl^- than for Br^- possibly because of the higher affinity of Cu(I) for chlorides with respect to bromides [12].

The presence of methyl acrylate has a drastic effect on the characteristics of the catalytic system: the copper complexes are significantly weaker reducing agents in this media (see Table 1) than in DMSO and also k_{act} is about one order of magnitude smaller in MA/DMSO than in DMSO. Also in this reaction media k_{act} decreases in the presence of X^-, again the effect being on average higher with Cl^- than in the case of Br^-.

One of the most employed initiators in RDRP reactions carried out in the presence of Cu^0 is ethyl 2-bromoisobutyrate, EBiB. We examined the kinetics of activation of this initiator by Cu(I). In both DMSO and MA/DMSO and with either ligand, TPMA or Me_6TREN, the reaction turned out to be too fast for the determination of k_{act} by the experimental technique used in this study. Monitoring the decay of Cu(I) oxidation current at RDE revealed that the reaction lasted in less than 1 s, which is of the same order of the time required to mix the reagents. The rate constant of the reaction could not be determined but a lower limit provided by the sensibility of the method can be set as $k_{act} > 5 \times 10^3\ M^{-1}\ s^{-1}$.

The kinetics of activation of alkyl halide initiators by Cu(I) complexes have been investigated by several research groups [13,51,56-58]. Unfortunately, almost all reported data are in acetonitrile and/or refer to RX/catalyst combinations different from those considered in this study. Therefore, direct comparison of the k_{act} values reported here with literature data is not possible. A general comparison between literature data in CH_3CN [13,56] and the results of this study shows that activation of RX is ca 2 orders of magnitude faster in DMSO than in CH_3CN, in agreement with a recent work on the effect of solvent on k_{act} [57]. The activation rate constants measured for methyl chloropropionate (MCP) in this work may be compared with k_{act} values reported for the activation of methyl bromopropionate (MBP) by $Cu^{I}Br/Me_6$TREN in DMSO and MA/DMSO 2/1 (v/v). Although in general bromides are more reactive than their corresponding chlorides [51,56], the k_{act} value reported for MBP ($3.2 \times 10^2\ M^{-1}\ s^{-1}$ in DMSO [42]) is unexpectedly smaller than that of MCP activation in similar reaction conditions, i.e. MCP + $[Cu^{I}Me_6TREN]^+ + Cl^-$ (see Table 4, entry 4). The value of k_{act} measured in this study in DMSO ($1.77 \times 10^3\ M^{-1}\ s^{-1}$) is in line with a previously reported k_{act} of $2.1 \times 10^3\ M^{-1}\ s^{-1}$ for MBP in CH_3CN [51], if one considers that k_{act} values in CH_3CN are roughly 2 orders of magnitude smaller than in DMSO [57]. On the other hand, the value of k_{act} reported for the activation of MBP by $Cu^{I}Br/Me_6$TREN in DMSO ($3.2 \times 10^2\ M^{-1}\ s^{-1}$) is comparable with $2.5 \times 10^2\ M^{-1}\ s^{-1}$ recently reported by Zerk and Bernhardt [58] for the activation of MBP by $Cu^{I}Br$/PMDETA, which, as a catalyst, is much less active than $Cu^{I}Br/Me_6$TREN [56]. It appears that $3.2 \times 10^2\ M^{-1}\ s^{-1}$ is too low for k_{act} of MBP + $Cu^{I}Br/Me_6$TREN in DMSO. k_{act} of the reaction between MBP and $Cu^{I}Br/Me_6$TREN has also been measured by Peng et al. [42] in MA/DMSO 2:1 (v/v). In this case, the value they report, $2.0 \times 10^2\ M^{-1}\ s^{-1}$, is as expected significantly greater than the rate constant we found for MCP activation in similar conditions (Table 4, entry 4).

Table 4
Activation rate constants, k_{act}, for the reaction between $[Cu^{I}L]^+$ and RX, in DMSO and MA/DMSO 2/1 (v/v) + 0.1 M Et_4NBF_4 at 25 °C. $C_{Cu(I)} = 5 \times 10^{-4}$ M, $C_{Cu(I)}:C_L:C_{RX}:C_{TEMPO} = 1:1.1:1:20$. Accuracy ± 5%.

Entry	L	RX	X^-[a]	$k_{act}/M^{-1}\ s^{-1}$	
				DMSO	MA/DMSO 2/1
1	Me_6TREN	EBA	–	1.78×10^3[b]	1.16×10^2
2	Me_6TREN	EBA	Br^-	1.14×10^3[b]	3.76×10^1
3	Me_6TREN	MCP	–	1.77×10^3[b]	1.21×10^2
4	Me_6TREN	MCP	Cl^-	6.15×10^2[b]	2.26×10^1[c]
5	Me_6TREN	BC	–	2.12×10^2[b]	1.57×10^1[c]
6	Me_6TREN	BC	Cl^-	6.17×10^1	1.61[c]
7	TPMA	MCP	–	5.40×10^1[d]	3.19×10^1[c]
8	TPMA	MCP	Cl^-	5.25[d]	9.29[c]

[a] Added as Et_4NCl or Et_4NBr; when present $C_{X^-}:C_{Cu(I)} = 2:1$.
[b] $C_{Cu(I)} = 2.5 \times 10^{-4}$ M.
[c] $C_{Cu(I)}:C_L:C_{RX}:C_{TEMPO} = 1:1.1:20:20$, pseudo first order conditions.
[d] $C_{Cu(I)} = 10^{-3}$ M.

3.4. Considerations on SET-LRP vs. SARA-ATRP mechanisms

Fig. 7 shows a schematic representation of two mechanisms, SARA ATRP and SET-LRP, proposed for RDRP reactions in the presence of Cu^0. To allow for a better comparison between the mechanisms, the scheme focuses on the role of copper, omitting all other aspects of the reaction such as generation, propagation and termination of radicals. Both mechanisms recognize that Cu^0 starts the process by reacting with the initiator RX to generate $R^\bullet$, but they completely disagree on the fate of Cu(I) produced in this reaction. According to SET-LRP, Cu(I) undergoes fast and complete disproportionation to Cu(II) and "nascent" Cu^0, which reacts rapidly with RX. Thus, Cu^0 is the exclusive activator of alkyl halides, whereas the principal role of Cu(I) is to regenerate highly reactive "nascent" Cu^0 through disproportionation; its role as activator is negligible. In contrast, SARA ATRP considers the process to be substantially like a conventional ATRP: the activation/deactivation equilibrium involves the Cu(I)/Cu(II) couple. So, Cu(I) is the principal activator of RX while Cu^0, besides being a supplemental activator, mainly regenerates Cu(I) through comproportionation.

It has been shown that Cu(I) is much more reactive than metallic copper toward activation of alkyl halides [42], so that if both copper species are present, RX will mainly react with Cu(I). Indeed, the kinetic comparison should consider the so-called "nascent" Cu^0, which might be more reactive than bulk copper. However, this species must be generated in solution by disproportionation of Cu(I). Therefore, the overall reaction route to be compared with reaction (11) is

$$2[Cu^{I}L]^+ \rightleftharpoons [Cu^{II}L]^{2+} + Cu^0 + L \quad (16)$$

$$Cu^0 + RX + L \rightleftharpoons [XCu^{I}L] + R^\bullet \quad (17)$$

where reaction (16) is just an example of the several possible disproportionation reactions. Note that it is pointless to compare the rate of reaction (17) with that of RX activation by Cu(I) since the overall rate of activation by Cu^0 cannot be higher than the rate of its formation. The rate constants reported in Tables 2–4 show that in most of the investigated systems ($[Cu^{I}L]^+$/RX/solvent), k_{act} is

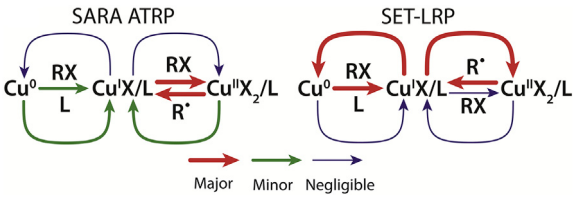

Fig. 7. Schematic representation of the role of copper in SARA ATRP (left) and SET-LRP (right) mechanisms. Major, minor and negligible reactions are indicated with arrows of decreasing size.

significantly greater than k_{disp}. In particular, if one considers the catalytic system mainly employed in RDRP reactions in the presence of Cu^0, that is, $[Cu^{I}Me_6TREN]^+$ as catalyst, EBiB as initiator and DMSO as solvent, it is found that k_{act} is at least 3 orders of magnitude greater than k_{disp}. Although these data alone provide a clear evidence that the reaction sequence represented by reactions (16) and (17) can be neglected in comparison with reaction (11), it is better to use rates, v, rather than rate constants. If we express the rates of Cu(I) disproportionation and RX activation by Cu(I) as

$$v_{disp} = k_{disp} C^2_{Cu(I)} \tag{18}$$

$$v_{act} = k_{act} C_{Cu(I)} C_{RX} \tag{19}$$

the ratio between the rates of the two reactions is given by

$$\frac{v_{act}}{v_{disp}} = \frac{k_{act} C_{RX}}{k_{disp} C_{Cu(I)}} \tag{20}$$

In a well-controlled RDRP process, the concentration of the dormant species is close to that of the initiator, i.e. $C_{RX} \approx C^0_{RX}$. On the other hand, when Cu^0 is used as the activator, Cu(I) is initially absent; it is formed during the process but its concentration rises to a very small stationary state value. A typical value of C^0_{RX} is 0.03 M [59-62]. Estimation of the stationary state concentration of Cu(I) is more difficult. The overall quantity of dissolved copper in the presence of Cu^0 does not exceed the amount of free ligand initially added to the system, which is typically 10% of the initiator. If we assume that the amount of copper complex present in solution is the maximum allowed by the ligand concentration and 10% of the dissolved copper is Cu(I), we can estimate $C_{Cu(I)}$ as 3×10^{-4} M. This value is in line with estimates of $C_{Cu(I)}$ reported in the literature for RDRP with Cu^0 [44,63].

Fig. 8 shows v_{act}/v_{disp} values calculated for all investigated systems on the basis of the above described assumptions together with the measured k_{act} and k_{disp} values. Although these values might be underestimated because of the chosen $C_{Cu(I)}$ value, they give a clear picture of the fate of Cu(I). Disproportionation is at least more than 2 orders of magnitude slower than RX activation. If we consider $v_{act}/v_{disp} = 10^2$ as the lowest limit required to neglect disproportionation with respect to activation (horizontal plane in Fig. 8), we observe that all investigated systems have values well beyond this limit. Additionally, if we consider the catalytic system most frequently used in RDRP with Cu^0, i.e. Me_6TREN with EBiB as initiator, the ratio of the rates becomes $v_{act}/v_{disp} > 5 \times 10^3$. These data show that once Cu(I) is formed from the initial activation by Cu^0, it hardly goes back to Cu^0 as disproportionation is outrun by reaction of Cu(I) with the dormant alkyl halide. This is a clear evidence of the inconsistency of the SET-LRP mechanism, which assumes fast and complete disproportionation of Cu(I) to Cu(II) and Cu(0). The results support the SARA ATRP mechanism, which considers Cu(I) to be the principal activator, with Cu^0 playing the role of a reducing agent for Cu(II) and a supplemental activator of RX. This conclusion is based on kinetic data obtained in typical polymerization conditions, but we wish to note that the competition parameter might be significantly affected if drastic conditions greatly enhancing k_{disp} are employed. For example, if a large quantity of a finely divided Cu^0 powder is used, k_{disp} may be greatly enhanced through surface catalysis. However, whether such an enhancement would result in a v_{act}/v_{disp} ratio smaller than 1 needs to be experimentally proved.

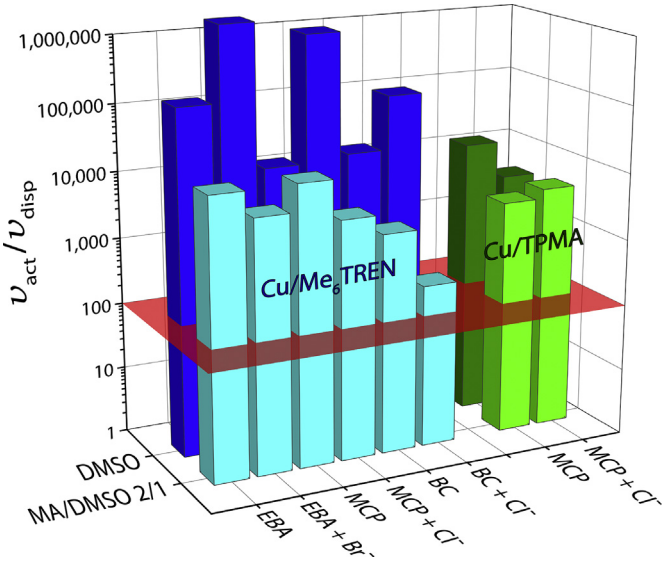

Fig. 8. v_{act}/v_{disp} ratio for all investigated complex/ligand combinations.

3.5. Conclusions

A comparative kinetic study on disproportionation of Cu(I) and its reaction with alkyl halides provides a decisive evidence on the fate of Cu(I), shedding some light on the mechanism of RDRP in the presence of metallic copper. Considering a series of alkyl halides used as initiators and two copper complexes in DMSO and MA/DMSO, it is found that $k_{act} > k_{disp}$. In particular, if the typical experimental conditions often employed for RDRP catalyzed by Cu^0 are considered, i.e. $[Cu^{I}Me_6TREN]^+$ with ethyl 2-bromoisobutyrate in DMSO, k_{act} is found to be more than 3 orders of magnitude greater than k_{disp}. This indicates that Cu(I) almost exclusively disappears through reaction with RX, with negligible contribution from disproportionation. The competition is found to be even more favorable to RX activation if, instead of the rate constants, the reaction rates are considered. Rough estimates of v_{act}/v_{disp}, based on the measured rate constants and estimated stationary state concentrations of RX and Cu(I), show that disproportionation is by no means competitive with RX activation. Therefore, the SET-LRP assumption that Cu(I) exclusively undergoes disproportionation cannot be correct. Cu^0 is not the exclusive activator, with Cu(I) involved in a fast disproportionation reaction to regenerate Cu^0 as assumed by SET-LRP. The data obtained in this study support the other way around: the principal role of Cu(I) is to activate RX, disproportionation being negligible. This is in line with SARA ATRP and proves the inconsistency of SET-LRP.

Acknowledgment

Financial support from the University of Padova is gratefully acknowledged.

References

[1] Jenkins AD, Jones RG, Moad G. Terminology for reversible-deactivation radical polymerization previously called “controlled” radical or “living” radical polymerization (IUPAC recommendations 2010). Pure Appl Chem 2010;82:483–91.
[2] Goto A, Fukuda T. Kinetics of living radical polymerization. Prog Polym Sci 2004;29:329–85.
[3] Matyjaszewski K, Davis TP. Handbook of radical polymerization. Hoboken, New Jersey: John Wiley & Sons, Inc.; 2002.
[4] Braunecker WA, Matyjaszewski K. Controlled/living radical polymerization: features, developments, and perspectives. Prog Polym Sci 2007;32:93–146.
[5] Kato M, Kamigaito M, Sawamoto M, Higashimura T. Polymerization of methyl methacrylate with the carbon tetrachloride/dichlorotris- (triphenylphosphine)ruthenium(II)/methylaluminum bis(2,6-di-tert-butylphenoxide)

initiating system: possibility of living radical polymerization. Macromolecules 1995;28:1721–3.
[6] Wang J-S, Matyjaszewski K. Controlled/"living" radical polymerization. Atom transfer radical polymerization in the presence of transition-metal complexes. J Am Chem Soc 1995;117:5614–5.
[7] Matyjaszewski K. Atom transfer radical polymerization (ATRP): current status and future perspectives. Macromolecules 2012;45:4015–39.
[8] Kamigaito M, Ando T, Sawamoto M. Metal-catalyzed living radical polymerization. Chem Rev 2001;101:3689–746.
[9] Matyjaszewski K, Xia J. Atom transfer radical polymerization. Chem Rev 2001;101:2921–90.
[10] Percec V, Guliashvili T, Ladislaw JS, Wistrand A, Stjerndahl A, Sienkowska MJ, et al. Ultrafast synthesis of ultrahigh molar mass polymers by metal-catalyzed living radical polymerization of acrylates, methacrylates, and vinyl chloride mediated by SET at 25 °C. J Am Chem Soc 2006;128:14156–65.
[11] Rosen BM, Percec V. Single-electron transfer and single-electron transfer degenerative chain transfer living radical polymerization. Chem Rev 2009;109:5069–119.
[12] Bortolamei N, Isse AA, Di Marco V, Gennaro A, Matyjaszewski K. Thermodynamic properties of copper complexes used as catalysts in atom transfer radical polymerization. Macromolecules 2010;43:9257–67.
[13] De Paoli P, Bortolamei N, Isse AA, Gennaro A. New insights into the mechanism of activation of atom transfer radical polymerization by Cu(I) complexes. Chem Commun 2011;47:3580–2.
[14] Matyjaszewski K, Tsarevsky NV, Braunecker WA, Dong H, Huang J, Jakubowski W, et al. Role of Cu^0 in controlled/"living" radical polymerization. Macromolecules 2007;40:7795–806.
[15] Jakubowski W, Matyjaszewski K. Activators regenerated by electron transfer for atom-transfer radical polymerization of (meth)acrylates and related block copolymers. Angew Chem Int Ed 2006;45:4482–6.
[16] Jakubowski W, Min K, Matyjaszewski K. Activators regenerated by electron transfer for atom transfer radical polymerization of styrene. Macromolecules 2006;39:39–45.
[17] Matyjaszewski K, Jakubowski W, Min K, Tang W, Huang JY, Braunecker WA, et al. Diminishing catalyst concentration in atom transfer radical polymerization with reducing agents. Proc Natl Acad Sci USA 2006;103:15309–14.
[18] D'Hooge DR, Konkolewicz D, Reyniers MF, Marin GB, Matyjaszewski K. Kinetic modelling of ICAR ATRP. Macromol Theor Simul 2012;21:52–69.
[19] Magenau AJD, Strandwitz NC, Gennaro A, Matyjaszewski K. Electrochemically mediated atom transfer radical polymerization. Science 2011;332:81–4.
[20] Bortolamei N, Isse AA, Magenau AJD, Gennaro A, Matyjaszewski K. Controlled aqueous atom transfer radical polymerization with electrochemical generation of the active catalyst. Angew Chem Int Ed 2011;50:11391–4.
[21] Magenau AJD, Bortolamei N, Frick E, Park S, Gennaro A, Matyjaszewski K. Investigation of electrochemically mediated atom transfer radical polymerization. Macromolecules 2013;46:4346–53.
[22] Tasdelen MA, Uygun M, Yagci Y. Photoinduced controlled radical polymerization in methanol. Macromol Chem Phys 2010;211:2271–5.
[23] Mosnáček J, Ilčíková M. Photochemically mediated atom transfer radical polymerization of methyl methacrylate using ppm amounts of catalyst. Macromolecules 2012;45:5859–65.
[24] Konkolewicz D, Schröder K, Buback J, Bernhard S, Matyjaszewski K. Visible light and sunlight photoinduced ATRP with ppm of Cu catalyst. ACS Macro Lett 2012;1:1219–23.
[25] Forsand BP, Hawker CJ. Control of living radical polymerization of methacrylates by light. Angew Chem Int Ed 2012;51:8850–3.
[26] Matyjaszewski K, Coca S, Gaynor SG, Wei M, Woodworth BE. Zerovalent metals in controlled/"living" radical polymerization. Macromolecules 1997;30:7348–50.
[27] Konkolewicz D, Wang Y, Zhong M, Krys P, Isse AA, Gennaro A, et al. Reversible-deactivation radical polymerization in the presence of metallic copper. A critical assessment of the SARA ATRP and SET-LRP mechanisms,. Macromolecules 2013;46:8749–72.
[28] Lligadas G, Percec V. SET-LRP of acrylates in the presence of radical inhibitors. J Polym Sci Part A: Polym Chem 2008;46:3174–81.
[29] Jiang X, Fleischmann S, Nguyen NH, Rosen BM, Percec V. The disproportionation of Cu(I)X mediated by ligand and solvent into Cu^0 and $Cu(II)X_2$ and its implications for SET-LRP. J Polym Sci Part A: Polym Chem 2009;47:5591–605.
[30] Fleischmann S, Percec V. SET-LRP of methyl methacrylate initiated with CCl4 in the presence and absence of air. J Polym Sci Part A: Polym Chem 2010;48:2243–50.
[31] Fleischmann S, Percec V. Copolymerization of methacrylic acid with methyl methacrylate by SET-LRP. J Polym Sci Part A: Polym Chem 2010;48:4884–8.
[32] Fleischmann S, Percec V. Set-LRP of MMA in acetic acid. J Polym Sci Part A: Polym Chem 2010;48:4889–93.
[33] Harrisson S, Couvreur P, Nicolas J. Simple and efficient copper metal-mediated synthesis of alkoxyamine initiators. Polym Chem 2011;2:1859–65.
[34] Wang W, Zhao J, Zhou N, Zhu J, Zhang W, Pan X, et al. Reversible deactivation radical polymerization in the presence of zero-valent metals: from components to precise polymerization. Polym Chem 2014;5:3533–46.
[35] Levere ME, Willoughby I, O'Donohue S, de Cuendias A, Grice AJ, Fidge C, et al. Assessment of SET-LRP in DMSO using online monitoring and rapid GPC. Polym Chem 2010;1:1086–94.
[36] Boyer C, Atme A, Waldron C, Anastasaki A, Wilson P, Zetterlund PB, et al. Copper(0)-mediated radical polymerisation in a self-generating biphasic system. Polym Chem 2013;4:106–12.
[37] Magenau AJD, Kwak Y, Matyjaszewski K. ATRP of methacrylates utilizing CuIIX2/L and copper wire. Macromolecules 2010;43:9682–9.
[38] Kwak Y, Magenau AJD, Matyjaszewski K. ARGET ATRP of methyl acrylate with inexpensive ligands and ppm concentrations of catalyst. Macromolecules 2011;44:811–9.
[39] Isse AA, Gennaro A, Yeh Lin C, Hodgson JL, Coote ML, Guliashvili T. Mechanism of carbon–halogen bond reductive cleavage in activated alkyl halide initiators relevant to living radical polymerization: theoretical and experimental study. J Am Chem Soc 2011;133:6254–64.
[40] Konkolewicz D, Krys P, Gois JR, Mendonca PV, Zhong M, Wang Y, et al. Aqueous RDRP in the presence of Cu^0: the exceptional activity of CuI confirms the SARA ATRP mechanism. Macromolecules 2014;47:560–70.
[41] Wang Y, Zhong M, Zhu W, Peng C-H, Zhang Y, Konkolewicz D, et al. Reversible-deactivation radical polymerization in the presence of metallic copper. Comproportionation–disproportionation equilibria and kinetics. Macromolecules 2013;46:3793–802.
[42] Peng C-H, Zhong M, Wang Y, Kwak Y, Zhang Y, Zhu W, et al. Reversible-deactivation radical polymerization in the presence of metallic copper. Activation of alkyl halides by Cu^0. Macromolecules 2013;46:3803–15.
[43] Zhang N, Samanta SR, Rosen BM, Percec V. Single electron transfer in radical ion and radical-mediated organic, materials and polymer synthesis. Chem Rev 2014;114:5848–958.
[44] Konkolewicz D, Wang Y, Krys P, Zhong M, Isse AA, Gennaro A, et al. SARA ATRP or SET-LRP. End of controversy? Polym Chem 2014;5:4396–417.
[45] Cardinale A, Isse AA, Gennaro A, Robert M, Savéant J-M. Dissociative electron transfer to haloacetonitriles. An example of the dependency of in-cage ion-radical interactions upon the leaving group. J Am Chem Soc 2002;124:13533–9.
[46] Isse AA, Gennaro A. Homogeneous reduction of haloacetonitriles by electrogenerated aromatic radical anions: determination of the reduction potential of $^{\bullet}CH_2CN$. J Phys Chem A 2004;108:4180–6.
[47] Percec V, Popov AV, Ramirez-Castillo E, Weichold O. Living radical polymerization of vinyl chloride initiated with iodoform and catalyzed by nascent Cu^0/tris(2-aminoethyl)amine or polyethyleneimine in water at 25 °C proceeds by a new competing pathways mechanism. J Polym Sci Part A – Polym Chem 2003;41:3283–99.
[48] Zhang Q, Wilson P, Li Z, McHale R, Godfrey J, Anastasaki A, et al. Aqueous copper-mediated living polymerization: exploiting rapid disproportionation of CuBr with Me6TREN. J Am Chem Soc 2013;135:7355–63 [and references therein].
[49] Nguyen NH, Levere ME, Kulis J, Monteiro MJ, Percec V. Analysis of the Cu0-catalyzed polymerization of methyl acrylate in disproportionating and non-disproportionating solvents. Macromolecules 2012;45:4606–22.
[50] Gahler AR. Colorimetric determination of copper with neo-cuproine. Anal Chem 1954;26:577–9.
[51] Isse AA, Bortolamei N, De Paoli P, Gennaro A. On the mechanism of activation of copper-catalyzed atom transfer radical polymerization. Electrochim Acta 2013;110:655–62.
[52] Qiu J, Matyjaszewski K, Thouin L, Amatore C. Cyclic voltammetric studies of copper complexes catalyzing atom transfer radical polymerization. Macromol Chem Phys 2000;201:1625–31.
[53] Bard AJ, Faulkner RL. Electrochemical methods. 2nd ed. New York: John Wiley & Sons; 2001.
[54] Skene WG, Scaiano JC, Listigovers NA, Kazmaier PM, Georges MK. Rate constants for the trapping of various carbon-centered radicals by nitroxides: unimolecular initiators for living free radical polymerization. Macromolecules 2000;33:5065–72.
[55] Lebedev NV, Zubenko DP, Bagryanskaya EG, Sagdeev RZ, Ananchenko GS, Marque S, et al. Switched external magnetic field CIDNP studies of coupling reaction of carbon-centered radicals with TEMPO. Phys Chem Chem Phys 2004;6:2254–9.
[56] Tang W, Matyjaszewski K. Effects of initiator structure on activation rate constants in ATRP. Macromolecules 2007;40:1858–63.
[57] Horn M, Matyjaszewski K. Solvent effects on the activation rate constant in atom transfer radical polymerization. Macromolecules 2013;46:3350–7.
[58] Zerk TJ, Bernhardt PV. New method for exploring deactivation kinetics in copper-catalyzed atom transfer radical reactions. Inorg Chem 2014;53:11351–3.
[59] Zhang Y, Wang Y, Peng C-H, Zhong M, Zhu W, Konkolewicz D, et al. Copper-mediated CRP of methyl acrylate in the presence of metallic copper: effect of ligand structure on reaction kinetics. Macromolecules 2012;45:78–86.
[60] Nguyen NH, Percec V. Dramatic acceleration of SET-LRP of methyl acrylate during catalysis with activated Cu^0 wire. J Polym Sci Part A: Polym Chem 2010;48:5109–19.
[61] Levere ME, Nguyen NH, Percec V. No reduction of $CuBr_2$ during Cu^0-catalyzed living radical polymerization of methyl acrylate in DMSO at 25 °C. Macromolecules 2012;45:8267–74.
[62] Nguyen NH, Kulis J, Sun H-J, Jia Z, van Beusekom B, Levere ME, et al. A comparative study of the SET-LRP of oligo(ethylene oxide) methyl ether acrylate in DMSO and in H_2O. Polym Chem 2013;4:144–55.
[63] Zhong Y, Wang Y, Krys P, Konkolewicz D, Matyjaszewski K. Reversible-deactivation radical polymerization in the presence of metallic copper. Kinetic simulation. Macromolecules 2013;46:3816–27.